Fully gapped superconductivity in single crystals of noncentrosymmetric Re_6Zr with broken time-reversal symmetry

G. M. Pang,[1] Z. Y. Nie,[1] A. Wang,[1] D. Singh,[2] W. Xie,[1] W. B. Jiang,[1] Y. Chen,[1] R. P. Singh,[2] M. Smidman,[1,*] and H. Q. Yuan[1,3,†]

[1]*Center for Correlated Matter and Department of Physics, Zhejiang University, Hangzhou 310058, China*
[2]*Department of Physics, Indian Institute of Science Education and Research Bhopal, Bhopal 462066, India*
[3]*Collaborative Innovation Center of Advanced Microstructures, Nanjing 210093, China*

(Received 20 March 2018; revised manuscript received 23 May 2018; published 7 June 2018)

The noncentrosymmetric superconductor Re_6Zr has attracted much interest due to the observation of broken time-reversal symmetry in the superconducting state. Here we report an investigation of the superconducting gap structure of Re_6Zr single crystals by measuring the magnetic penetration depth shift $\Delta\lambda(T)$ and electronic specific heat $C_e(T)$. $\Delta\lambda(T)$ exhibits an exponential temperature dependence behavior for $T \ll T_c$, which indicates a fully open superconducting gap. Our analysis shows that a single gap s-wave model is sufficient to describe both the superfluid density $\rho_s(T)$ and $C_e(T)$ results, with a fitted gap magnitude larger than the weak coupling BCS value, providing evidence for fully gapped superconductivity in Re_6Zr with moderate coupling.

DOI: 10.1103/PhysRevB.97.224506

I. INTRODUCTION

Noncentrosymmetric superconductors (NCS) have attracted a great deal of attention due to the influence of antisymmetric spin-orbit coupling (ASOC) on the superconducting properties, which is induced by the antisymmetric potential gradient arising due to broken inversion symmetry [1,2]. Strong ASOC may lift the spin degeneracy of the conduction bands, allowing for superconducting states which are an admixture of spin-singlet and spin-triplet pairing, giving rise to a variety of unique properties [1–4]. Unconventional superconductivity was evidenced in the first heavy fermion NCS $CePt_3Si$, where a linear temperature dependence of the magnetic penetration depth at low temperatures and a constant Knight shift across T_c were observed [5,6]. While studies of heavy fermion NCS revealed a range of unusual findings, disentangling the role played by broken inversion symmetry from the effects of strong electronic correlations and magnetism is highly challenging, which spurred an interest in looking for weakly correlated NCS with singlet-triplet mixing. Evidence for such an admixture was demonstrated in $Li_2(Pd,Pt)_3B$, where Li_2Pd_3B has a fully open gap [7–9], but the gap of Li_2Pt_3B exhibits line nodes [9–11]. This change from nodeless to nodal superconductivity upon switching Pd for Pt was explained using a model with a mixture of singlet and triplet states, where there is a relative increase in the size of the spin-triplet component of the order parameter, as the ASOC is increased [9]. The Knight shift also shows a marked difference between the two compounds, corresponding to a decrease of the spin susceptibility below T_c for Li_2Pd_3B, while for Li_2Pt_3B this remains constant, indicating greater influence of the ASOC on the superconductivity [8,10].

Subsequently, the order parameters of a wider range of NCS have been studied, where evidence for nodal superconductivity was also found in quasi-one-dimensional $K_2Cr_3As_3$ [12] and the low carrier system YPtBi [13]. Meanwhile, although studies of Y_2C_3 at higher temperatures were accounted for by fully gapped superconductivity [14–16], very low temperature penetration depth measurements also indicate the presence of a nodal gap structure [17]. However, most NCS have been found to be fully gapped superconductors, such as $BaPtSi_3$ [18], BiPd [19–22], $PbTaSe_2$ [23–25], La_7Ir_3 [26], and Re_6Zr [27–30]. In particular, many NCS have been found compatible with single-gap s-wave superconductivity, indicating that the size of any triplet component is very small, and the relationship between the ASOC strength and the degree of singlet-triplet pairing is not entirely understood. Moreover, it has been proposed that some NCS can exhibit topological superconductivity. Both theoretical calculations and experimental studies reveal topological surface states in the NCS $PbTaSe_2$ and BiPd [20,31–33], which may lead to possible Majorana fermions in the vortex cores when these states are sufficiently close to the Fermi level.

Another notable feature of several NCS is the breaking of time-reversal symmetry (TRS). While broken TRS was previously discovered in the unconventional triplet superconductor Sr_2RuO_4 [34,35], evidence for this phenomenon has also been found in a number of NCS with fully gapped superconducting states, such as $LaNiC_2$ [36], La_7Ir_3 [26], and Re_6Zr [27]. In the case of $LaNiC_2$, the symmetry analysis shows that for TRS to be broken at T_c, the effect of the ASOC on the superconductivity should be weak, indicating a lack of significant mixed parity pairing [37]. On the other hand, Re_6Zr crystallizes in the cubic α-Mn structure, where the presence of three-dimensional irreducible representations of the point group potentially allows for TRS breaking with singlet-triplet mixing [27]. It is therefore of particular importance to characterize the superconducting order parameter of Re_6Zr. Previous

*msmidman@zju.edu.cn
†hqyuan@zju.edu.cn

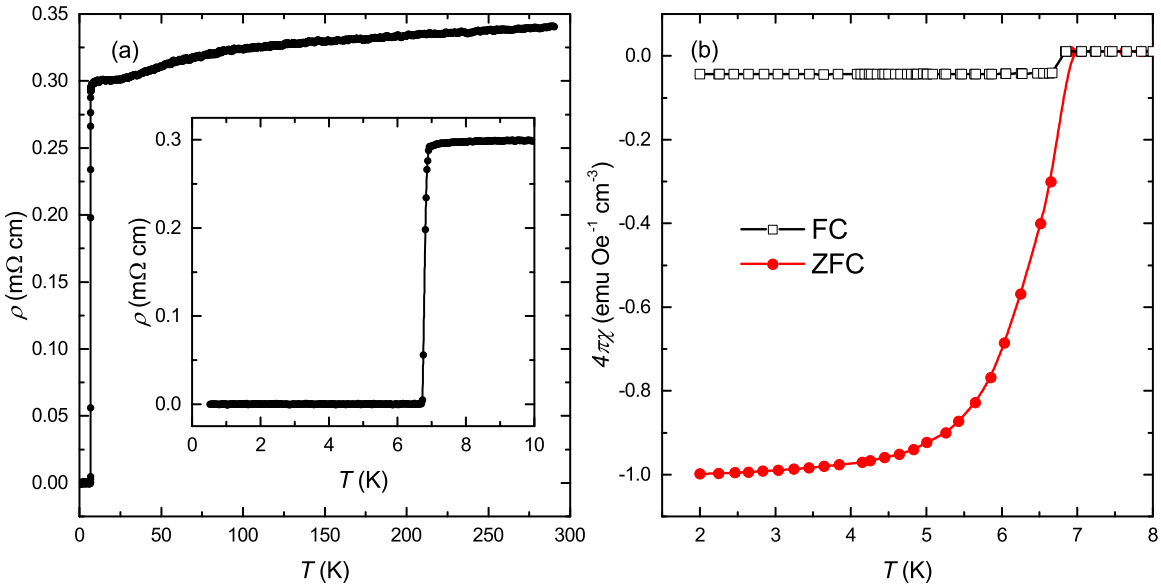

FIG. 1. Characterization of Re_6Zr single crystals showing the temperature dependence of (a) the electrical resistivity $\rho(T)$ from room temperature down to 0.3 K, and (b) the magnetic susceptibility $4\pi\chi$ between 2 and 8 K, where both field-cooled (FC) and zero-field-cooled curves in an applied field of 10 Oe are displayed. The inset of (a) shows an enlargement of $\rho(T)$ around $T_c = 6.8$ K.

measurements of the gap structure of polycrystalline samples are accounted for by nodeless single gap s-wave superconductivity [27–30], but different conclusions are drawn from recent point contact spectroscopy results from single crystal measurements, which give evidence for multiple gaps [38]. As such, it is important to perform further measurements of Re_6Zr single crystals sensitive to low energy excitations to clarify this issue. In this paper we study the superconducting order parameter of single crystalline Re_6Zr by measuring the magnetic penetration depth and specific heat of single crystals, which are both consistent with a single nodeless isotropic gap with a moderate coupling strength.

II. EXPERIMENTAL DETAILS

Single crystals of Re_6Zr were synthesized using the Czochralski method, as described in Ref. [38]. Magnetization measurements were performed using a superconducting quantum interference device (SQUID) magnetometer (MPMS) with both field cooling (FC) and zero-field cooling (ZFC), with a small applied magnetic field of 10 Oe. The electrical resistivity $\rho(T)$ was measured by using a standard four-probe method from room temperature down to 0.3 K in a ^{3}He refrigerator. The specific heat $C(T)$ was measured using a Physical Property Measurement System (PPMS) with a ^{3}He insert down to around 0.6 K. The temperature dependence of the magnetic penetration depth shift $\Delta\lambda(T) = \lambda(T) - \lambda(0)$ was measured using a tunnel-diode-oscillator (TDO) technique in a ^{3}He cryostat down to 0.35 K. The operating frequency of the TDO setup is about 7 MHz, with a noise level as low as 0.1 Hz. For the TDO measurements, the sample was cut into a regular shape with dimensions of $700\times500\times200$ μm^3 and mounted onto a sapphire rod so that it may be placed into the coil without making contact. The sample experiences a very small ac field of about 20 mOe along the [100] direction induced by the coil, which is much smaller than the lower critical field H_{c1}, ensuring that the sample remains in the Meissner state, so that the change of the magnetic penetration depth $\Delta\lambda(T)$ is proportional to the frequency change $\Delta f(T) = f(T) - f(0)$. Here $\Delta\lambda(T) = G\Delta f(T)$, where the calibration constant G is determined by the geometry of the sample and coil [39].

III. RESULTS AND DISCUSSION

Single crystals of Re_6Zr were characterized by the measurements of the electrical resistivity $\rho(T)$ and magnetic susceptibility $4\pi\chi(T)$, which are displayed in Fig. 1. $\rho(T)$ exhibits metallic behavior in the normal state with a residual resistivity of $\rho(7\text{ K}) = 0.3$ mΩ cm, just above the superconducting transition. This yields a mean free path of 2.1 nm [40], with a coherence length of $\xi = 5.5$ nm deduced from the upper critical field, and a Sommerfeld coefficient of $\gamma_n = 27.4$ mJ mol^{-1} K^{-2} from our specific heat measurements described below. The calculated mean free path is less than half the coherence length, indicating that the sample is closer to the dirty limit. The inset of Fig. 1(a) displays an enlargement of $\rho(T)$ at low temperatures, where a sharp superconducting transition occurs at $T_c = 6.8$ K, with a transition width less than 0.2 K. In addition, the temperature dependence of the magnetic susceptibility in Fig. 1(b) shows that the zero-field-cooled (ZFC) curve exhibits full diamagnetism, providing evidence for bulk superconductivity in the Re_6Zr single crystals.

Figure 2 displays the temperature dependence of the penetration depth shift $\Delta\lambda(T)$ at low temperatures from TDO-based measurements. The frequency change $\Delta f(T)$ is plotted in the inset from about 7.5 K down to the base temperature of 0.35 K, which has been normalized by the normal state value. Here a sharp superconducting transition occurs at around 6.8 K, in line with the resistivity, and magnetic susceptibility measurements. $\Delta\lambda(T)$ decreases rapidly upon reducing the temperature, before becoming flat below around 1.5 K, indicating a fully open superconducting gap in Re_6Zr. For an s-wave superconductor,

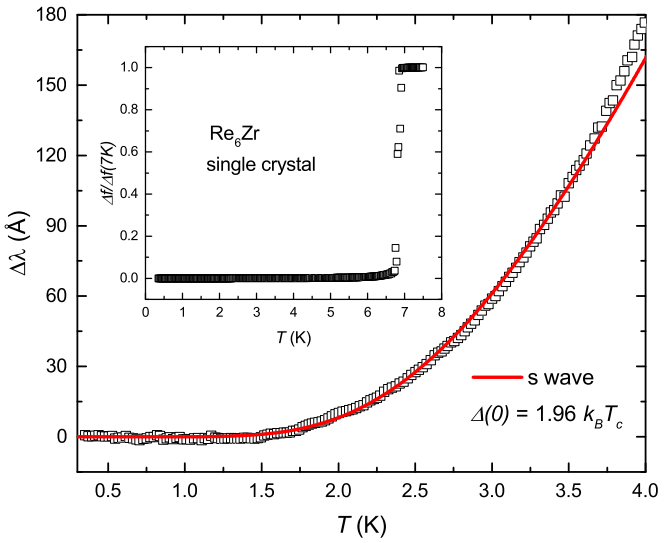

FIG. 2. Temperature dependence of the penetration depth shift $\Delta\lambda(T)$ at low temperatures, where exponential behavior is observed. The solid red line displays the fitted curve for an s-wave model with $\Delta(0) = 1.96\, k_B T_c$. The inset shows the frequency shift from 7.5 down to 0.35 K, normalized by the 7 K value, which displays a sharp superconducting transition at $T_c = 6.8$ K.

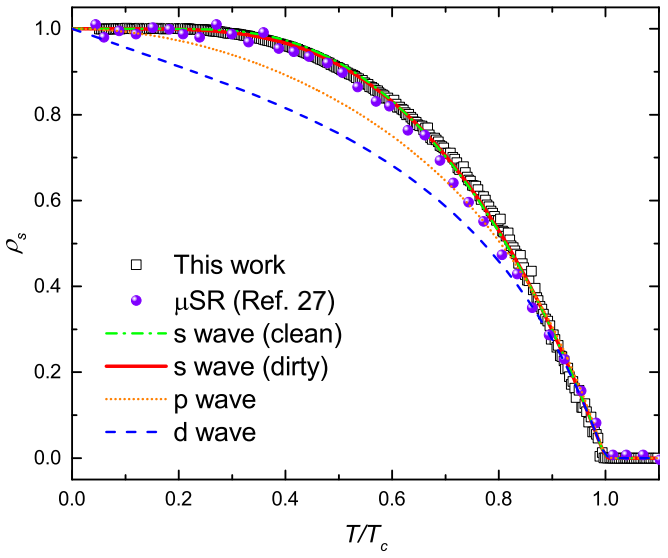

FIG. 3. Normalized superfluid density $\rho_s(T)$, as a function of the reduced temperature T/T_c. The black squares are the data from this work, while the dots are from μSR results in Ref. [27]. The lines show the superfluid density calculated from various models of the gap structure.

the change of magnetic penetration depth shows exponentially activated behavior at $T \ll T_c$, as

$$\Delta\lambda(T) = \lambda(0)\left[\sqrt{\frac{\pi\Delta(0)}{2k_BT}}\exp\left(-\frac{\Delta(0)}{k_BT}\right)\right], \qquad (1)$$

where $\lambda(0)$ and $\Delta(0)$ are the penetration depth and superconducting gap magnitude at zero temperature, respectively. As shown by the solid red line, our experimental data can be well described by a single s-wave gap with $\lambda(0) = 200$ nm and $\Delta(0) = 1.96\, k_B T_c$. The value of $\lambda(0)$ and the temperature dependence of $\Delta\lambda(T)$ are comparable with those in Ref. [29], suggesting that both single crystal and polycrystalline samples are consistent with a similar nodeless gap structure. We note that for a superconductor with line nodes in the dirty limit, a quadratic dependence would be expected at low temperatures instead of a linear $\Delta\lambda(T)$ [41]. However, upon analyzing with a power-law dependence $\Delta\lambda(T) \propto T^n$, values of n of 4.4 and 6.1 are obtained fitting from the base temperature up to 3 and 2.2 K, respectively. Since these exponents are significantly larger than two, such a dirty nodal scenario can be ruled out.

Moreover the magnetic penetration depth was also converted into the normalized superfluid density via $\rho_s = [\lambda(0)/\lambda(T)]^2$, which is displayed as a function of the reduced temperature T/T_c in Fig. 3. For a clean superconductor, $\rho_s(T)$ can be calculated using

$$\rho_s(T) = 1 + 2\left\langle\int_{\Delta_k}^{\infty}\frac{EdE}{\sqrt{E^2-\Delta_k^2}}\frac{\partial f}{\partial E}\right\rangle_{FS}, \qquad (2)$$

where $f(E,T) = [1+\exp(E/k_BT)]^{-1}$ is the Fermi-Dirac distribution function and the superconducting gap function is defined as $\Delta_k(T) = \Delta(T)g_k$. This contains an angular dependent part g_k and a temperature dependent component $\Delta(T)$, which can be approximated as $\Delta(T) = \Delta(0)\tanh\{1.82[1.018(T_c/T-1)]^{0.51}\}$ [42]. Here the zero temperature gap magnitude $\Delta(0)$ is the only fitted parameter. As shown by the green dashed-dotted line in Fig. 3, a single gap s-wave model with $g_k = 1$ can well reproduce the experimental data with $\Delta(0) = 2.23\, k_B T_c$. This gap magnitude is larger than the value of $1.76\, k_B T_c$ for weakly coupled BCS superconductors, suggesting moderately strong coupling in Re_6Zr. On the other hand, since as discussed above the samples are near to the dirty limit, a dirty s-wave model was also applied, where $\rho_s(T) = \frac{\Delta(T)}{\Delta(0)}\tanh[\frac{\Delta(T)}{2k_BT}]$ [43]. The results are shown by the solid red line, which also well accounts for the experimental data with $\Delta(0) = 2.1\, k_B T_c$. In order to compare with nodal superconducting scenarios, both a p-wave model with $g_k = \sin\theta$ and a d-wave model $g_k = \cos 2\phi$ are also displayed, where θ is the polar angle and ϕ is the azimuthal angle. It is obvious that the superfluid density of p- and d-wave superconductors change significantly with temperature, even at very low temperatures, which is in contrast with the data showing near temperature independence below around $0.25\, T_c$. Furthermore, we also compare our results with measurements of polycrystalline samples using transverse-field muon-spin rotation (μSR) measurements from Ref. [27]. These are displayed in Fig. 3 and show that comparable superconducting gap structures are inferred from measurements of single crystal and polycrystalline samples.

The specific heat measurements of Re_6Zr single crystals were also analyzed to further characterize the superconducting order parameter. In the inset of Fig. 4, the total specific heat as C/T is displayed, which contains both electronic and phonon contributions. In the normal state, the data were fitted using $C(T) = \gamma_n T + \beta T^3 + \delta T^5$, where $C_e = \gamma_n T$ and $C_{ph} = \beta T^3 + \delta T^5$ represent the electron and phonon contributions, respectively, and γ_n is the Sommerfeld coefficient. The fitting

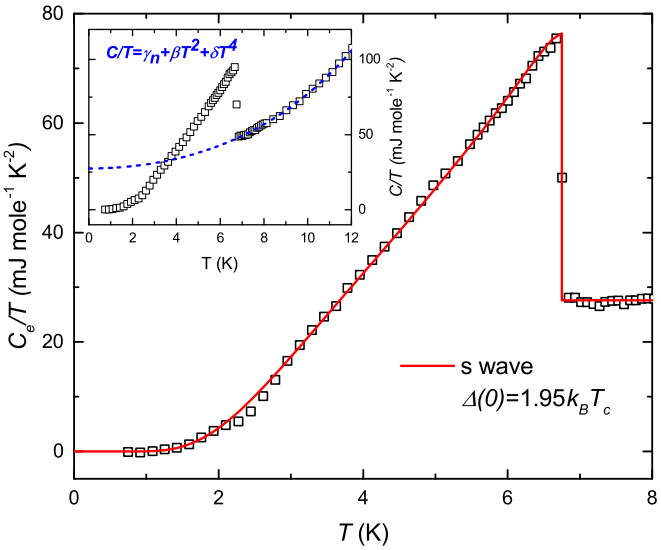

FIG. 4. Temperature dependence of the electronic specific heat as $C_e(T)/T$ of single crystalline Re_6Zr. The solid red line represents the fitting results from a single gap s-wave model. The inset displays the total $C(T)/T$, where the dashed line shows the fit to the normal state.

results are shown by the dashed line with fitted parameters of $\beta = 0.39$ mJ mol^{-1} K^{-4}, $\delta = 1$ μJ mol^{-1} K^{-6}, and $\gamma_n = 27.4$ mJ mol^{-1} K^{-2}, which are consistent with measurements of polycrystalline samples [27].

The main panel of Fig. 4 displays the temperature dependence of the electronic specific heat as C_e/T in the superconducting state after subtracting the phonon contribution. A sizable jump is observed around T_c of $\Delta C/\gamma_n T_c = 1.76$, which is larger than the value of 1.43 for a weakly coupled BCS superconductor, again indicating an enhancement of the coupling strength in Re_6Zr. In the superconducting state, the entropy S can be expressed as [44]

$$S = -\frac{3\gamma_n}{\pi^3}\int_0^{2\pi}\int_0^{\infty}[f\ln f + (1-f)\ln(1-f)]d\varepsilon d\phi \quad (3)$$

and therefore the electronic specific heat in the superconducting state can be calculated as $C_e = TdS/dT$. Due to $C_e(T)/T$ becoming flat with decreasing temperature for $T \ll T_c$, the data were fitted using an isotropic s-wave model, and the results are shown in Fig. 4 by the solid red line. It can be clearly seen that this model well describes the experimental data, with a fitted parameter of $\Delta(0) = 1.95\ k_B T_c$. This is consistent with the penetration depth and superfluid density results and also indicates a moderately enhanced superconducting gap magnitude.

Since Re_6Zr is a NCS, the ASOC will lift the spin degeneracy of the electron bands, which can potentially give rise to a mixture of spin singlet and spin triplet pairing states, leading to a two-gap structure $\Delta_\pm = \psi \pm |\mathbf{d}|$, where ψ and $\mathbf{d}$ represent the singlet and triplet components [1]. Therefore the experimental results being consistent with a single nodeless gap implies that the spin triplet component is very small relative to the spin singlet. The origin of TRS breaking in Re_6Zr still remains difficult to account for. In $LaNiC_2$, because of the low symmetry of the orthorhombic crystal structure, the breaking of TRS at T_c implies that singlet-triplet mixing is weak, and moreover that the pairing corresponds to a nonunitary triplet state [36,37]. Here the lack of a role played by ASOC was corroborated by the breaking of TRS in the similar but centrosymmetric $LaNiGa_2$ [45], and the observation of two-gap superconductivity in both $LaNiC_2$ and $LaNiGa_2$ allowed for the proposal of a nodeless even-parity, nonunitary triplet state, where the overall pairing wave function is antisymmetric upon particle exchange due to an antisymmetric orbital index [46]. Such a scenario is not readily applied to Re_6Zr, since the higher symmetry of the cubic α-Mn crystal structure lifts the constraint that TRS breaking at T_c must correspond to nonunitary pairing, and moreover most studies only show evidence for single-gap behavior. As the symmetry analysis of Re_6Zr also allows for mixed singlet-triplet pairing with broken TRS [27], further studies are highly desirable to understand the origin of TRS breaking and the role of the ASOC in the superconducting state of Re_6Zr.

IV. CONCLUSIONS

To summarize, we have measured the magnetic penetration depth and electronic specific heat of single crystals of the noncentrosymmetric superconductor Re_6Zr. Exponential behavior of $\Delta\lambda(T)$ was observed at $T \ll T_c$, which indicates the absence of low energy excitations, and a fully gapped superconducting state. Both the superfluid density and specific heat can be well accounted for by a single gap s-wave model across the whole temperature range with a gap magnitude larger than the weak coupling BCS value, providing strong evidence for fully gapped superconductivity with moderately strong coupling in Re_6Zr.

ACKNOWLEDGMENTS

We thank X. Lu for helpful discussions and suggestions. This work was supported by the National Natural Science Foundation of China (No. 11474251, No. U1632275), the National Key R&D Program of China (No. 2017YFA0303100, No. 2016YFA0300202), and the Science Challenge Project of China (No. TZ2016004). R.P.S. acknowledges the Science and Engineering Research Board, Government of India for the Young Scientist Grant No. YSS/2015/001799.

[1] M. Smidman, M. B. Salamon, H. Q. Yuan, and D. F. Agterberg, Superconductivity and spin-orbit coupling in non-centrosymmetric materials: A review, Rep. Prog. Phys. **80**, 036501 (2017).

[2] E. Bauer and M. Sigrist, *Non-Centrosymmetric Superconductors: Introduction and Overview*, Lecture Notes in Physics (Springer, Berlin, 2012).

[3] L. P. Gorkov and E. I. Rashba, Superconducting 2D System with Lifted Spin Degeneracy: Mixed Singlet-Triplet State, Phys. Rev. Lett. **87**, 037004 (2001).

[4] P. A. Frigeri, D. F. Agterberg, A. Koga, and M. Sigrist, Superconductivity without Inversion Symmetry: MnSi versus $CePt_3Si$, Phys. Rev. Lett. **92**, 097001 (2004).

[5] I. Bonalde, W. Bramer-Escamilla, and E. Bauer, Evidence for Line Nodes in the Superconducting Energy Gap of Noncentrosymmetric $CePt_3Si$ from Magnetic Penetration Depth Measurements, Phys. Rev. Lett. **94**, 207002 (2005).

[6] M. Yogi, H. Mukuda, Y. Kitaoka, S. Hashimoto, T. Yasuda, R. Settai, T. D. Matsuda, Y. Haga, Y. Onuki, P. Rogl, and E. Bauer, Evidence for novel pairing state in noncentrosymmetric superconductor $CePt_3Si$: ^{29}Si-NMR Knight shift study, J. Phys. Soc. Jpn. **75**, 013709 (2006).

[7] H. Takeya, K. Hirata, K. Yamaura, K. Togano, M. El Massalami, R. Rapp, F. A. Chaves, and B. Ouladdiaf, Low-temperature specific-heat and neutron-diffraction studies on Li_2Pd_3B and Li_2Pt_3B superconductors, Phys. Rev. B **72**, 104506 (2005).

[8] M. Nishiyama, Y. Inada, and G.-Q. Zheng, Superconductivity of the ternary boride Li_2Pd_3B probed by ^{11}B NMR, Phys. Rev. B **71**, 220505(R) (2005).

[9] H. Q. Yuan, D. F. Agterberg, N. Hayashi, P. Badica, D. Vandervelde, K. Togano, M. Sigrist, and M. B. Salamon, *S*-Wave Spin-Triplet Order in Superconductors without Inversion Symmetry: Li_2Pd_3B and Li_2Pt_3B, Phys. Rev. Lett. **97**, 017006 (2006).

[10] M. Nishiyama, Y. Inada, and G.-Q. Zheng, Spin Triplet Superconducting State due to Broken Inversion Symmetry in Li_2Pt_3B, Phys. Rev. Lett. **98**, 047002 (2007).

[11] H. Takeya, M. ElMassalami, S. Kasahara, and K. Hirata, Specific-heat studies of the spin-orbit interaction in noncentrosymmetric $Li_2(Pd_{1-x}Pt_x)_3B$ ($x = 0,0.5,1$) superconductors, Phys. Rev. B **76**, 104506 (2007).

[12] G. M. Pang, M. Smidman, W. B. Jiang, J. K. Bao, Z. F. Weng, Y. F. Wang, L. Jiao, J. L. Zhang, G. H. Cao, and H. Q. Yuan, Evidence for nodal superconductivity in quasi-one-dimensional $K_2Cr_3As_3$, Phys. Rev. B **91**, 220502(R) (2015).

[13] H. Kim, K. Wang, Y. Nakajima, R. Hu, S. Ziemak, P. Syers, L. Wang, H. Hodovanets, J. D. Denlinger, P. M. R. Brydon, D. F. Agterberg, M. A. Tanatar, R. Prozorov, and J. Paglione, Beyond triplet: Unconventional superconductivity in a spin-3/2 topological semimetal, Sci. Adv. **4**, eaao4513 (2018).

[14] A. Harada, S. Akutagawa, Y. Miyamichi, H. Mukuda, Y. Kitaoka, and J. Akimitsu, Multigap superconductivity in Y_2C_3: A 13C-NMR study, J. Phys. Soc. Jpn. **76**, 023704 (2007).

[15] S. Akutagawa and J. Akimitsu, Superconductivity of Y_2C_3 investigated by specific heat measurement, J. Phys. Soc. Jpn. **76**, 024713 (2007).

[16] S. Kuroiwa, Y. Saura, J. Akimitsu, M. Hiraishi, M. Miyazaki, K. H. Satoh, S. Takeshita, and R. Kadono, Multigap Superconductivity in Sesquicarbides La_2C_3 and Y_2C_3, Phys. Rev. Lett. **100**, 097002 (2008).

[17] J. Chen, M. B. Salamon, S. Akutagawa, J. Akimitsu, J. Singleton, J. L. Zhang, L. Jiao, and H. Q. Yuan, Evidence of nodal gap structure in the noncentrosymmetric superconductor Y_2C_3, Phys. Rev. B **83**, 144529 (2011).

[18] E. Bauer, R. T. Khan, H. Michor, E. Royanian, A. Grytsiv, N. Melnychenko-Koblyuk, P. Rogl, D. Reith, R. Podloucky, E. W. Scheidt, W. Wolf, and M. Marsman, $BaPtSi_3$: A noncentrosymmetric BCS-like superconductor, Phys. Rev. B **80**, 064504 (2009).

[19] K. Matano, S. Maeda, H. Sawaoka, Y. Muro, T. Takabatake, B. Joshi, S. Ramakrishnan, K. Kawashima, J. Akimitsu, and G.-Q. Zheng, NMR and NQR studies on non-centrosymmetric superconductors Re_7B_3, LaBiPt, and BiPd, J. Phys. Soc. Jpn. **82**, 084711 (2013).

[20] Z. Sun, M. Enayat, A. Maldonado, C. Lithgow, E. Yelland, D. C. Peets, A. Yaresko, A. P. Schnyder, and P. Wahl, Dirac surface states and nature of superconductivity in noncentrosymmetric BiPd, Nat. Commun. **6**, 6633 (2015).

[21] L. Jiao, J. L. Zhang, Y. Chen, Z. F. Weng, Y. M. Shao, J. Y. Feng, X. Lu, B. Joshi, A. Thamizhavel, S. Ramakrishnan, and H. Q. Yuan, Anisotropic superconductivity in noncentrosymmetric BiPd, Phys. Rev. B **89**, 060507(R) (2014).

[22] X. B. Yan, Y. Xu, L. P. He, J. K. Dong, H. Cho, D. C. Peets, J.-G. Park, and S. Y. Li, Nodeless superconductivity in the noncentrosymmetric superconductor BiPd, Supercond. Sci. Technol. **29**, 065001 (2016).

[23] C.-L. Zhang, Z. Yuan, G. Bian, S.-Y. Xu, X. Zhang, M. Z. Hasan, and S. Jia, Superconducting properties in single crystals of the topological nodal semimetal $PbTaSe_2$, Phys. Rev. B **93**, 054520 (2016).

[24] G. M. Pang, M. Smidman, L. X. Zhao, Y. F. Wang, Z. F. Weng, L. Q. Che, Y. Chen, X. Lu, G. F. Chen, and H. Q. Yuan, Nodeless superconductivity in noncentrosymmetric $PbTaSe_2$ single crystals, Phys. Rev. B **93**, 060506 (2016).

[25] M. X. Wang, Y. Xu, L. P. He, J. Zhang, X. C. Hong, P. L. Cai, Z. B. Wang, J. K. Dong, and S. Y. Li, Nodeless superconducting gaps in noncentrosymmetric superconductor $PbTaSe_2$ with topological bulk nodal lines, Phys. Rev. B **93**, 020503(R) (2016).

[26] J. A. T. Barker, D. Singh, A. Thamizhavel, A. D. Hillier, M. R. Lees, G. Balakrishnan, D McK. Paul, and R. P. Singh, Unconventional Superconductivity in La_7Ir_3 Revealed by Muon Spin Relaxation: Introducing a New Family of Noncentrosymmetric Superconductor That Breaks Time-Reversal Symmetry, Phys. Rev. Lett. **115**, 267001 (2015).

[27] R. P. Singh, A. D. Hillier, B. Mazidian, J. Quintanilla, J. F. Annett, D. M. Paul, G. Balakrishnan, and M. R. Lees, Detection of Time-Reversal Symmetry Breaking in the Noncentrosymmetric Superconductor Re_6Zr Using Muon-Spin Spectroscopy, Phys. Rev. Lett. **112**, 107002 (2014).

[28] K. Matano, R. Yatagai, S. Maeda, and G.-Q. Zheng, Full-gap superconductivity in noncentrosymmetric Re_6Zr, $Re_{27}Zr_5$, and $Re_{24}Zr_5$, Phys. Rev. B **94**, 214513 (2016).

[29] M. A. Khan, A. B. Karki, T. Samanta, D. Browne, S. Stadler, I. Vekhter, A. Pandey, P. W. Adams, D. P. Young, S. Teknowijoyo, K. Cho, R. Prozorov, and D. E. Graf, Complex superconductivity in the noncentrosymmetric compound Re_6Zr, Phys. Rev. B **94**, 144515 (2016).

[30] D. A. Mayoh, J. A. T. Barker, R. P. Singh, G. Balakrishnan, D. McK. Paul, and M. R. Lees, Superconducting and normal-state properties of the noncentrosymmetric superconductor Re_6Zr, Phys. Rev. B **96**, 064521 (2017).

[31] G. Bian, T.-R. Chang, R. Sankar, S.-Y. Xu, H. Zheng, T. Neupert, C.-K. Chiu, S.-M. Huang, G. Q. Chang, I. Belopolski, D. S. Sanchez, M. Neupane, N. Alidoust, C. Liu, B. K. Wang, C.-C. Lee, H.-T. Jeng, C. L. Zhang, Z. J. Yuan, S. Jia, A. Bansil, F. C. Chou, H. Lin, and M. Z. Hasan, Topological nodal-line fermions in spin-orbit metal $PbTaSe_2$, Nat. Commun. **7**, 10556 (2016).

[32] S. Y. Guan, P. J. Chen, M. W. Chu, R. Sankar, F. Chou, H. T. Jeng, C. S. Chang, and T. M. Chuang, Superconducting topological surface states in the noncentrosymmetric bulk superconductor $PbTaSe_2$, Sci. Adv. **2**, e1600894 (2016).

[33] M. Neupane, N. Alidoust, M. M. Hosen, J.-X. Zhu, K. Dimitri, S.-Y. Xu, N. Dhakal, R. Sankar, I. Belopolski, D. S. Sanchez, T.-R. Chang, H.-T. Jeng, K. Miyamoto, T. Okuda, H. Lin, A. Bansil, D. Kaczorowski, F. C. Chou, M. Z. Hasan, and T. Durakiewicz, Observation of the spin-polarized surface state in a noncentrosymmetric superconductor BiPd, Nat. Commun. **7**, 13315 (2016).

[34] G. M. Luke, Y. Fudamoto, K. M. Kojima, M. I. Larkin, J. Merrin, B. Nachumi, Y. J. Uemura, Y. Maeno, Z. Q. Mao, Y. Mori *et al.*, Time-reversal symmetry-breaking superconductivity in Sr_2RuO_4, Nature (London) **394**, 558 (1998).

[35] J. Xia, Y. Maeno, P. T. Beyersdorf, M. M. Fejer, and A. Kapitulnik, High Resolution Polar Kerr Effect Measurements of Sr_2RuO_4: Evidence for Broken Time-Reversal Symmetry in the Superconducting State, Phys. Rev. Lett. **97**, 167002 (2006).

[36] A. D. Hillier, J. Quintanilla, and R. Cywinski, Evidence for Time-Reversal Symmetry Breaking in the Noncentrosymmetric Superconductor $LaNiC_2$, Phys. Rev. Lett. **102**, 117007 (2009).

[37] J. Quintanilla, A. D. Hillier, J. F. Annett, and R. Cywinski, Relativistic analysis of the pairing symmetry of the noncentrosymmetric superconductor $LaNiC_2$, Phys. Rev. B **82**, 174511 (2010).

[38] P. Parab, D. Singh, H. Muthurajan, R. P. Singh, P. Raychaudhuri, and S. Bose, Multiband superconductivity in the time reversal symmetry broken superconductor Re_6Zr, arXiv:1704.06166.

[39] R. Prozorov, R. W. Giannetta, A. Carrington, and F. M. Araujo-Moreira, Meissner-London state in superconductors of rectangular cross section in a perpendicular magnetic field, Phys. Rev. B **62**, 115 (2000).

[40] T. P. Orlando, E. J. McNiff, S. Foner, and M. R. Beasley, Critical fields, Pauli paramagnetic limiting, and material parameters of Nb_3Sn and V_3Si, Phys. Rev. B **19**, 4545 (1979).

[41] P. J. Hirschfeld and N. Goldenfeld, Effect of strong scattering on the low-temperature penetration depth of a d-wave superconductor, Phys. Rev. B **48**, 4219 (1993).

[42] A. Carrington and F. Manzano, Magnetic penetration depth of MgB_2, Physica C **385**, 205 (2003).

[43] M. Tinkham, *Introduction to Superconductivity*, 2nd ed. (McGraw Hill, New York, 1996).

[44] F. Bouquet, Y. Wang, R. A. Fisher, D. G. Hinks, J. D. Jorgensen, A. Junod, and N. E. Phillips, Phenomenological two-gap model for the specific heat of MgB_2, Europhys. Lett. **56**, 856 (2001).

[45] A. D. Hillier, J. Quintanilla, B. Mazidian, J. F. Annett, and R. Cywinski, Nonunitary Triplet Pairing in the Centrosymmetric Superconductor $LaNiGa_2$, Phys. Rev. Lett. **109**, 097001 (2012).

[46] Z. F. Weng, J. L. Zhang, M. Smidman, T. Shang, J. Quintanilla, J. F. Annett, M. Nicklas, G. M. Pang, L. Jiao, W. B. Jiang, Y. Chen, F. Steglich, and H. Q. Yuan, Two-Gap Superconductivity in $LaNiGa_2$ with Nonunitary Triplet Pairing and Even Parity Gap Symmetry, Phys. Rev. Lett. **117**, 027001 (2016).